

Blocked force investigation of a Terfenol-D transducer

Rick Kellogg^{*a}, Alison Flatau^{*b}

Aerospace Engineering and Engineering Mechanics, Iowa State University, Ames, IA 50011

ABSTRACT

The output force-strain relationship typical of the performance of Terfenol-D transducers under varied operating conditions is examined to study transducer blocked force characteristics. The design and construction of a transducer for testing under controlled thermal, magnetic and mechanical load conditions are described. Results of compression tests at various applied magnetic fields and two initial mechanical stress states are used to generate load lines and the blocked force characteristics of the transducer. Comparisons of the transducer's force and strain output are made with published data. This test data is also used to examine the variability in Young's Modulus with applied magnetic field, strain and stress.

Keywords: blocked force, Terfenol-D, magnetostriction, transducer, load-line, Young's Modulus

1. INTRODUCTION

Effective use of a transducer requires knowledge of its displacement and force outputs under a given input. Transducers utilizing the magnetostrictive alloy Terfenol-D are finding growing use, and a deeper grasp of their output characteristics is needed to improve modeling and control. The following investigation of a Terfenol-D transducer is intended to shed some light on the response of Terfenol-D drivers under quasi-static conditions. Quasi-static changes in transducer displacement and force output for different applied magnetic field inputs will be examined.

As a starting point in the transducer analysis, consider the output characteristics of an ideal linear transducer sketched in Figure 1. This represents a DC load line, where the transducer's ability to generate DC forces is linearly dependent on the displacement of the driving element. In particular, under no load (zero force produced) the transducer's displacement is maximized, while as the strain produced tends toward zero the transducer's ability to generate force is maximized. This maximum force may be termed as the "Blocked Force" rating of the transducer.

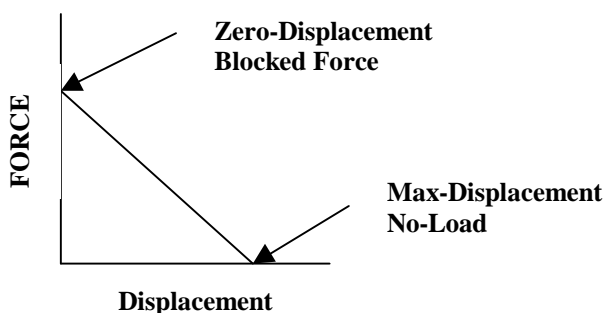


Figure 1. DC load line for an ideal transducer.

*a Correspondence: Email: rkellogg@iastate.edu; Telephone (515)294-0088; Fax (515)294-8584

*b Correspondence: Email: abf@iastate.edu; Telephone (515)294-0094; Fax (515)294-8584

Now consider a transducer with a Terfenol-D drive element. Terfenol-D is an alloy of Terbium, Iron, and Dysprosium.¹ This alloy undergoes magnetostriction or it strains in response to the application of a magnetic field, H .³ The magnetic domains of a Terfenol-D rod are oriented such that a magnetic field applied along the longitudinal axis of the rod causes the rod to elongate in the longitudinal direction. A simplified model of a transducer's quasi-static performance is given by the force-displacement relationship in Equation 1a, where, the force output of the transducer, F_T , is equal to the stiffness of the drive element, k_m , times its output displacement u_H .³ The displacement, u_H , is due to magnetostriction at an applied magnetic field H . Furthermore, the stiffness of the driving element may be modeled in Equation 1b where E_Y^H is the Terfenol-D Young's modulus at constant H , A is its cross sectional area and L its length.

$$F_T = k_m u_H \qquad k_m = E_Y^H \frac{A}{L} \qquad (1a,b)$$

Combining Equations 1a and 1b along with the substitution of the strain potential \mathbf{e} for u_H/L leads to the force strain relation in Equation 2a. The transducer's force output F_T is proportional to the drive element's Young's modulus and strain potential at an applied field H .

$$F_T = A E_Y^H \mathbf{e} \qquad (2a)$$

$$F_B^H = A E_Y^H \mathbf{e}_{\max}^H \qquad (2b)$$

Arguably, based on Equation 2a, the maximum force that can be developed in a transducer and hence its blocked force rating F_B^H can be established as a function of the maximum strain of the device under application of an applied field H as posed in Equation 2b. However the elastic modulus for Terfenol-D has been measured at values of between 12 and 120 GPa ($1.74 \cdot 10^6$ and $17.4 \cdot 10^6$ psi) depending on its stress state,⁴ its temperature,⁵ and the magnetic field applied to it.⁶

The experimental study described in the remainder of the paper was undertaken to better understand the effects of stress and applied magnetic field on the blocking force achievable in a Terfenol-D transducer. Section two of the paper discusses the transducer design used for testing under controlled thermal, magnetic and mechanical conditions, along with some of the factors related to obtaining accurate system response measurements. Transducer design considerations focused on providing careful control of experimental conditions and allowing for operation under constant temperatures, constant applied magnetic fields and/or constant compressive loads. Section 3 of the paper presents experimental results that provide a characterization of DC load lines and the blocked force output of the transducer based on data generated through compression tests. This section also includes experimental results reflecting the variations in the transducer's Terfenol-D drive element modulus of elasticity with operating conditions. This is followed by a comparison of the blocked force as predicted with Equation 2b to the measured blocked forces and a brief statement of project conclusions and future directions.

2. THE TRANSDUCER DESIGN

With the goal of testing the transducer under controlled conditions, transducer thermal, magnetic and mechanical operating regimes were considered. First, to provide thermal control, active cooling was incorporated to mitigate the effects of ohmic heating in the solenoid used to generate the applied magnetic fields. The design constraint used to address thermal control was the desire for steady state operation at 21 ± 1 °C (70 ± 2 °F) under a maximum applied magnetic field of 2400 Oersted. Second, it was necessary to utilize an efficient magnetic circuit to minimize heating, flux leakage, and to achieve an approximately uniform magnetic flux throughout the Terfenol-D core. Third, to allow flexibility for introducing mechanical loads to the transducer, the test system and transducer were designed to allow several methods for loading capabilities. Belleville spring washers within the transducer were used to pre-load of the Terfenol-D drive element,¹ external masses provided for constant force loading conditions, and a MTS machine was used to generate variable force loads. Finally, the ability to acquire accurate measurement of the transducer's magnetic states (applied field and core magnetic induction) and mechanical states (displacement and

force output) was needed. The magnetic field generated by the solenoid was monitored with a Hall probe and a sense coil measuring changes in magnetic induction within the Terfenol-D, both of which were built into the test transducer. A force transducer and an LVDT (linear variable differential transformer) were located in series and in parallel respectively with the transducer mechanical output (as opposed to, for example, a discrete local strain measurement using a resistance strain gage mounted on the Terfenol-D core). The transducer housing was designed to accommodate accurate instrumentation positioning.

A schematic of the transducer used for this study is shown below in Figure 2. A 6.35 mm ($\frac{1}{4}$ inch) diameter, 50.8 mm (2 in) long Terfenol-D ($Tb_{0.3}Dy_{0.7}Fe_{1.95}$) rod resides at the center of the transducer. Surrounding the Terfenol-D rod is a 486-turn two-layer sense coil. A Hall Effect chip (*Allegro 3516L*) was located at the midpoint of the rod length with its active region at 1.6 mm ($\frac{1}{16}$ in) to the side of the Terfenol-D. Exterior to the sense coil and Hall chip, is a solenoid for generating applied magnetic fields. The solenoid's innermost layer consists of quarter-inch outer diameter copper cooling tubes upon which were wound 600 turns of 15 gauge magnet wire. Another layer of cooling tubes and 600 turns of magnet wire followed. Finally, more copper cooling tube encased the sides, top, and bottom of the solenoid for thermal isolation from the Terfenol-D core and steel case. For the maximum magnetic fields used (2400 Oersted developed at 12 amps), a 3.78 liter/min (1 gal/min) flow rate of 20 °C (68° F) water was used to maintain a constant temperature at the Terfenol-D core. A Techron 7780 amplifier was used in current control mode to drive the solenoid at constant DC fields. Surrounding the solenoid, a steel casing serves to complete the magnetic circuit. The completed transducer was 114 mm (4.5 in) tall and 165 mm (6.5 in) in diameter. The entire transducer is supported on a 114 mm (4.5 in) thick aluminum base to minimize magnetic flux leakage into the steel frame of the compression test machine.

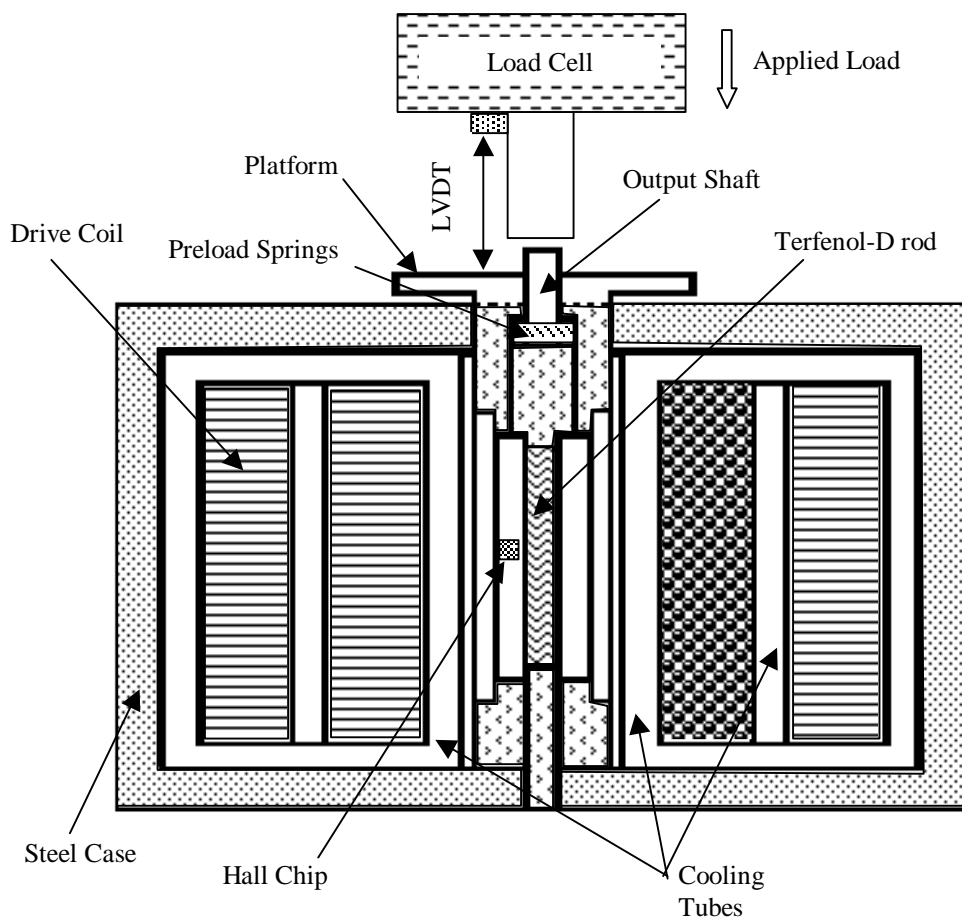


Figure 2. Transducer schematic.

Data acquisition was accomplished using a National Instruments DAQ Board along with LabView software running on a PC computer. Data was collected at a rate of 50 samples per second. The load cell and the LVDT outputs provided load and displacement information. The solenoid current and Hall Effect chip were sampled for the magnetic field and the sense coil for magnetic induction. The applied forces needed for testing were generated in two ways. Constant load tests involved free weights, and variable load tests utilized a MTS machine with a compressive displacement rate of 0.38 mm (15 mils) per minute.

3. RESULTS

BUTTERFLY CURVES Strain-applied field measurements were undertaken to characterize the transducer's output capability. The strain was measured with varying applied H under 0.0 and 6.9 MPa (0.0 and 1.0 ksi) free-weight preload (or prestress) conditions. Standard butterfly curves generated using a sinusoidal applied field H with a frequency of 0.2 Hz and amplitude of 2000 Oersted are shown in Fig. 3, indicating performance typical of commercially available Terfenol-D transducers. An expected feature of the butterfly curves is that the 6.9 MPa (1.0 ksi) preload condition develops strains approaching 1800 microstrain or nearly three times that of the 600 microstrain attained under the zero preload condition. The Terfenol-D rod's strain dependence on preload is due to pre-stress causing rotation of the rod's magnetic moments so that they are initially aligned perpendicular to the applied stress. This allows for larger achievable strains due to increased net moment rotation when an applied axial magnetic field causes the rod's moments to rotate and align with the axial magnetic field⁴. A 6.9 MPa (1.0 ksi) axial prestress is typically sufficient to provide an initial state in which these moments are predominantly perpendicular to the rod's longitudinal axis without introducing too much of a mechanical load against which work must be done to produce strain. (For more on this, see reference 7.)

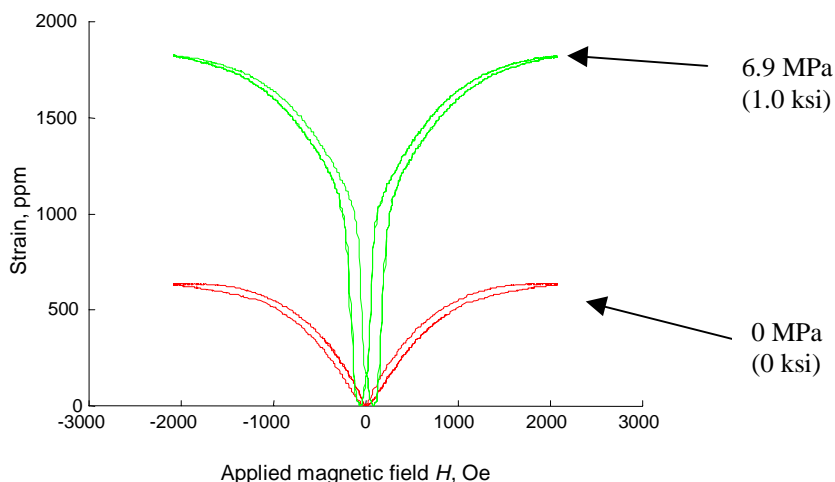


Figure 3. Butterfly curves for zero and 6.9 MPa (1.0 ksi) preload conditions.

LOAD LINES Next, generation of the transducer load lines is investigated. The testing procedure begins with demagnetization of the Terfenol-D sample under zero load, or a preload of $s_0 = 0.0$. Demagnetization was accomplished by applying a 0.2 Hz sinusoidal magnetic field, H , with an amplitude that decreased from 2000 Oe to zero over a period of 20 seconds. This demagnetization process was used to provide a reproducible demagnetized state for the start of each load line test. Following demagnetization, a constant applied field H is established and finally compression at a rate of 0.38 mm (15 mil) per minute was applied until a compressive load of 86.1 MPa (12.5 ksi) was achieved. Figure 4 shows a generic strain versus applied field trace of the testing process. It indicates a typical strain path under application of a DC magnetic field H , (strain increases from $e(s_0, 0)$ to $e(s_0, H)$), and the subsequent strain path under application of a 86.1 MPa (12.5 ksi) compressive force field, (strain decreases from $e(s_0, H)$ to $e(s_0 + 86.1 \text{ MPa}, H)$).

The load lines for a zero preload condition are shown in Figure 5 where stress (compressive force per the transducer's Terfenol-D core's cross sectional area) is plotted against strain for various DC applied magnetic fields. The maximum no-load strain for that constant DC magnetic field, H , is e_{max}^H . Under a constant applied magnetic field, as a compressive load is applied, stress in the transducer core increases while its strain capability decreases. These transducer load lines reflect higher forces at lower strains as suggested by the sketch in Figure 1. Increases in applied magnetic field shift the load lines upwards and to the right, reflecting both higher forces and higher strains, and that for a given strain value, an increase occurs in the force or stress that can be developed in the transducer core. Another way of stating this observation is that an increase in the magnetic energy *applied to* the device results in an increase in the mechanical energy that can be *sustained by* (or *developed in*) the device. This suggests that the maximum applied field that can be generated in the transducer will limit the blocked force rating for a given transducer.

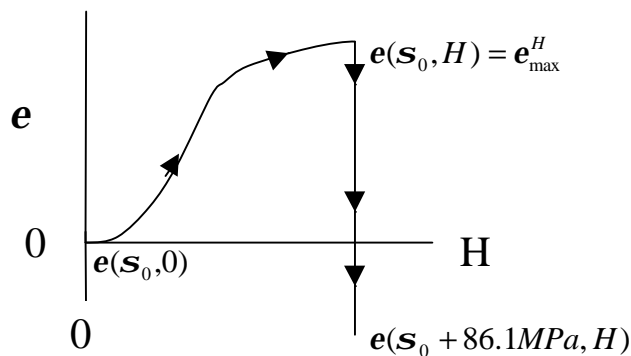


Figure 4. Path typical of changes in strain during a compression test.

In the region of positive strain ($e^H = 0$ to e_{max}^H), the load lines are fairly linear and in fact are roughly comparable to those of the ideal transducer depicted in Fig. 1. However as the Terfenol-D transducer core undergoes compression, (i.e. the negative strain region in Figure 5) the load lines become nonlinear. Ultimately, as the rod is compressed to strains exceeding -2000 microstrain, the load lines for all of the different applied field levels appear to asymptotically approach the linear trend bounded by the baseline curve reflecting compression under zero applied magnetic field. Note that the curve with no applied magnetic field behaves quite linearly under a compressive load of greater than roughly 7-10 MPa (1-1.5 ksi), after compression to roughly -1200 microstrain, reflecting the purely mechanical elastic properties of the transducer core⁸.

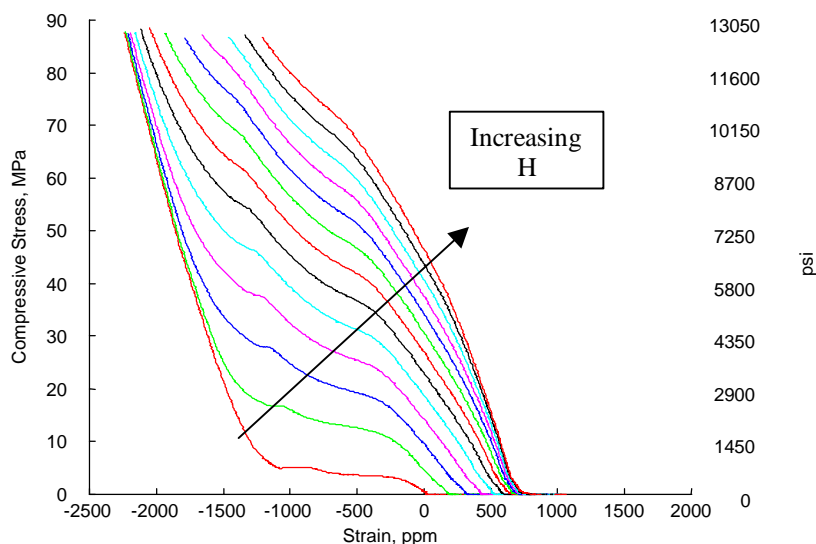


Figure 5. Zero preload load lines for applied field H from 0 - 2400 Oe at 200 Oe steps.

The transducer's Terfenol-D drive element has a yield strength of 700 MPa (101.5 ksi) in compression and 28.3MPa (4.1 ksi) in tension.¹ As a consequence, Terfenol-D transducers are operated almost exclusively under a compressive load. As noted, above an 86.1MPa (12.5 ksi) compressive load, it appears that the load lines asymptotically approach the linear curve generated by the purely mechanical stress-strain curve, i.e. the stress-strain test run under zero applied magnetic field. The slope of this asymptote tends toward approximately 110 GPa, which does correspond to a Young's Modulus for the Terfenol-D where mechanical effects dominate magnetic effects.¹

At this point we raise the issue of how and/or where on these load lines to define a blocked force rating. From Figure 5, a specific value for the blocked force rating for the transducer is not apparent, as this figure suggests that several criteria might be appropriate. For example, one could suggest that the blocked force rating should be equal to the maximum force generated by actively producing a positive strain in the device. Thus, the blocked force would be proportional to the compressive stress measured as the strain returns to zero (its initial length) under an increasing load. Alternatively, one could base a blocked force rating on the compressive stress above which an applied field no longer changes the load handling capability of the device from that of its purely mechanical compressive strength. In other words, the blocked force rating could be the force at which the various load lines asymptote to the purely mechanical stress-strain curve (the lower left-most curve). And finally, one could suggest that the ultimate compressive stress of the Terfenol-D driver reflects the maximum force that the device can undergo. Therefore, regardless of the applied field capability of the transducer, or alternatively given a large enough applied field, the Terfenol-D yield strength of 700MPa could be used to reflect the blocked force handling capability of the device.

For DC operation, it is quite reasonable to envision a device pushing against a load while under a negative strain. This suggests that it is appropriate to identify a blocked force as that force limit above which the applied magnetic field is no longer a factor in sustaining the force generated by the device. This would correspond to the force or stress value of the mechanical-only curve's data that the load line under a given constant applied field asymptotes toward. From Figure 5, the blocked force rating defined in this fashion would be roughly 34.5 MPa (5.0 ksi) or 1072 N (241 lb_f) for this device if its upper applied magnetic field generation capability was $H_{max} = 200$ Oe, 55.2 MPa (8.0 ksi) or 1720 N (386 lb_f) for $H_{max} = 400$ Oe, etc.

For AC operation, strains tend to be limited to positive strain excursions along either the left ($H < 0$) or right ($H > 0$) linear portion of butterfly curves such as those depicted in Figure 3. The driver core is unlikely to be compressed into a negative strain regime (other than that produced by an initial preload) without introducing significant nonlinearities in the transducer output. This suggests that it is appropriate to identify a blocked force as the force that would be generated at zero strain. Thus the blocked force rating would be 5.2 MPa (0.75 ksi) or 162 N (36 lb_f) if the transducer maximum field generation capability was 200 Oe, 44.1 MPa (6.4 ksi) or 1385 N (309 lb_f) for $H_{max} = 2400$ Oe, etc.

For the purpose of this study, blocked force F_B^H and blocked stress s_B^H are the force and stress developed in the transducer under a DC applied magnetic field H when the transducer's Terfenol-D driver has been compressed back to its preloaded length such that $e(s_{\theta} + s_B^H, H) = e(s_{\theta}, 0)$.

The mechanism of Terfenol-D's strain response to applied fields under different preloads has been widely studied^{4,9,10} and, for example, as suggested by the butterfly curves in Figure 3, one would expect a difference in the load lines generated for different preloads. Thus, for comparison with the 0.0 preload data, load line results for a 6.9 MPa (1.0 ksi) preload are presented in Figure 6.

These tests were conducted by applying the preload through compression of the Terfenol-D driver against Belleville spring washers and next demagnetizing the Terfenol-D core. A constant magnetic field was then applied followed by compression testing. An unfortunate consequence of the use of spring washers for providing preloads is that as the rod strains, an increase in load due to further compression of the spring washers occurs that is not accounted for in the forces detected by the MTS machine. Transducer designs that accommodate very soft spring washers can be used to minimize this effect. For the worst case studied, the ~1750 microstrain under 2400 Oe and no external mechanical load, the spring-induced prestress reaches 10.4 MPa (1.5 ksi) instead of the targeted 6.9 MPa (1.0 ksi), suggesting that at the higher strains, the load lines slightly under predict actual forces.

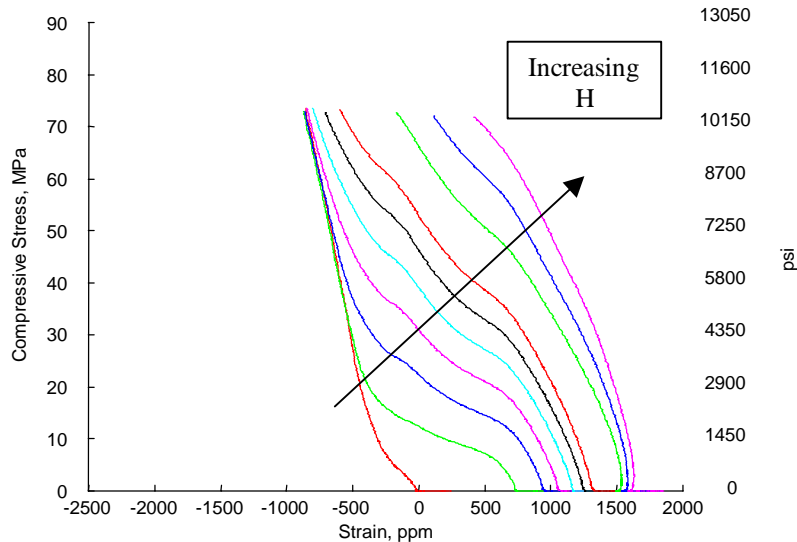


Figure 6. Load lines – 1.0 ksi preload, for applied H from 0 - 1200 Oe at 200 Oe steps and 1600, 2000, 2400 Oe.

The blocked force values obtained with the 6.9 MPa (1.0ksi) preload are approximately double those obtained with zero preload. However, it is interesting to note the similarities in the Figure 5 and 6 data. One can recognize mechanical-only curve in Figure 6 as the continuation of the mechanical-only curve in Figure 5 beyond where application of a 6.9 MPa (1.0 ksi) compressive mechanical load produced a -1200 microstrain compression. With only a slight change in slope of the entire data set and an offset relative to the actual zero magnetic field's zero force strain (i.e from $[0\mu\epsilon, 0\text{MPa}]$ in Fig. 6 to $[-1200\mu\epsilon, 8.0\text{MPa}]$ in Fig. 5), largely similar load line data trends can be seen in Figures 5 and 6.

In addition, both data sets exhibit a region in which the generally smooth load line slopes exhibit a localized fluctuation. This trend is exhibited between -500 and -1200 microstrain in Figure 5 and exhibited between roughly +500 to -200 microstrain in Figure 6. These strain regions actually coincide with respect to the net strain of the Terfenol-D transducer core after taking into account the strain of roughly 1000 to 1200 ppm (parts per million) introduced to the sample by the 6.9 MPa (1.0 ksi) preload.

The Hall probe output measured during the 0.0 preload compression tests are presented in Figure 7 and they also exhibit fluctuations from their nominally constant values over the same strain regions that the stress-strain slope fluctuations occur. (Because the Hall probe's upper limit for obtaining accurate measurements was 1000 Oe, Figure 7 shows data for only the 0-1000 Oe test cases.) Thus even this effect appears to indicate a correlation between the mechanical and magnetic effects within the transducer. Since the Hall probe is positioned to the side of the Terfenol-D rod, the probe's output is inversely related to the magnetic induction of the rod. The permeability changes of Terfenol-D with stress are governed by fairly complex magneto-mechanical coupling phenomena¹¹ for which accurate models are not yet readily implemented. Further testing using the transducer sense coil is underway to examine the hypothesis that a decrease in Terfenol-D's permeability coincides with the increases in the Hall probe output, and to relate this effect to variations in the Terfenol-D elastic modulus.

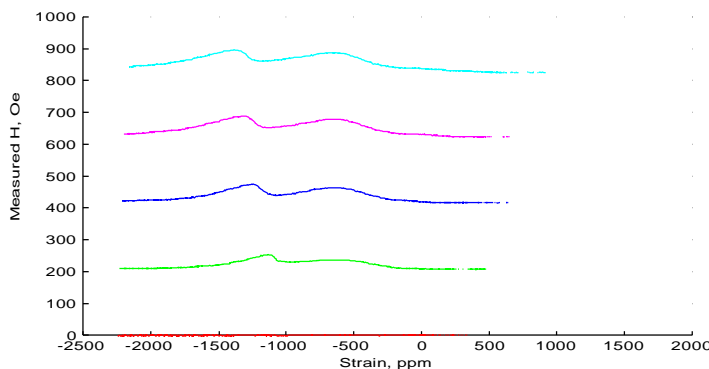


Figure 7. Hall probe output from zero preload compression tests.

It is interesting to compare the current data to data from similar tests of an alloy of slightly different stoichiometry collected using a similar test procedure by D. Pearson and collaborators⁸ for $Tb_{0.27}Dy_{0.73}Fe_2$. To reach a common format, the data in Figure 5 has been replotted with the sign of the strain reversed and the starting point for each load line offset to zero. The replotted data is shown in Figure 8a along side Pearson's data (as published in Butler's manual¹) in Figure 8b. The overall trend of the two plots is similar. Higher levels of applied magnetic field result in greater stress values for a given strain. However, unlike the newly collected data, no localized slope fluctuations occur, possibly indicating less jumping of magnetic moments from one easy axis to another and more uniform magnetic moment rotation associated with the differences in stoichiometry.

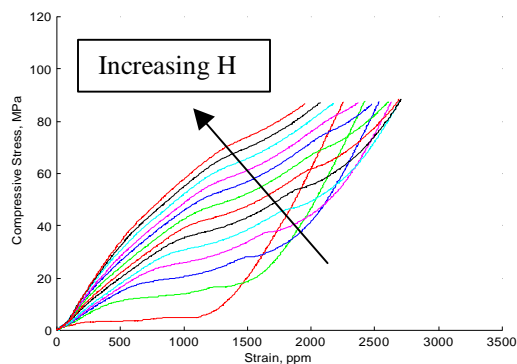


Figure 8a $Tb_{0.3}Dy_{0.7}Fe_{1.95}$ stress-strain data from Figure 5 (zero preload). Applied fields of 0-2400 Oe in 200 Oe increments.

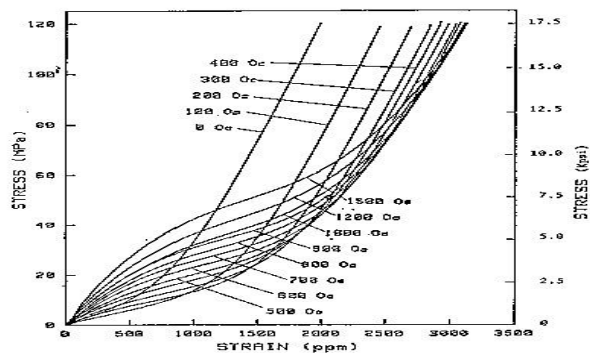


Figure 8b. $Tb_{0.27}Dy_{0.73}Fe_2$ stress-strain data from refs 1,8 (zero preload). Samples demagnetized to 0-1000 Oe in 100 Oe increments and 1200 and 1500 Oe.

ELASTIC MODULUS Additional information present in the load line data is that the slope of the stress-strain data provides a measure of the elastic modulus or Young's Modulus of the Terfenol-D core as it varies with operating conditions. Figures 9a and 9b show the modulus plotted as a function of strain for different DC applied magnetic fields with preloads of 0.0 and 6.9 MPa (0.0 and 1.0 ksi), respectively. The trends shown are similar to those published.^{1,8,12} In the most general sense, similar trends are observed in these two figures at strains differing by roughly 1200 ppm that are consistent with the prestress effects observed in Figure 3, and in the strain shift between Figures 5, and 6. The modulus is generally lower when realignment of magnetic moments most easily occurs, e.g. at compressive strains slightly below those produced by a compressive force of 6.9 MPa (1.0 ksi) in Figure 9a, and at strains associated with the burst region (the steeper portion of the butterfly curve) in Figure 9b.

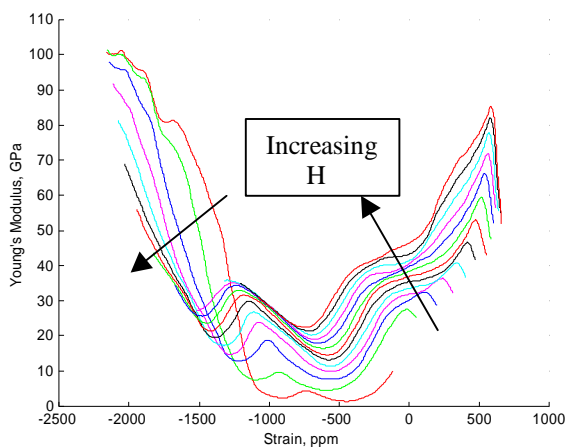


Figure 9a. Young's Modulus vs. strain, zero preload for fields of 0-2400 Oe at increments of 200 Oe.

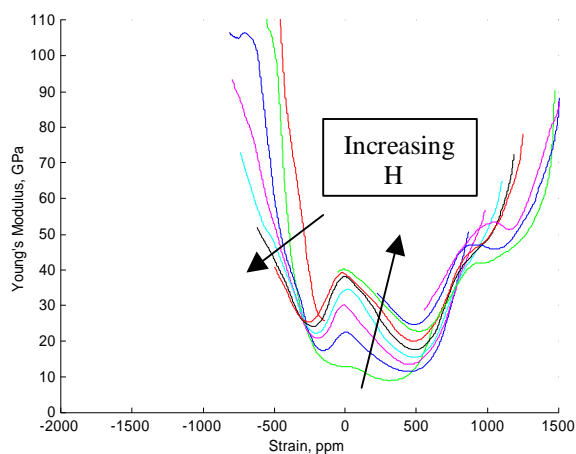


Figure 9b. Young's Modulus vs. strain, 6.9 MPa preload for fields of 0 - 1200 Oe at 200 Oe steps and 1600, 2000, 2400 Oe.

A second interesting trend observed in Figure 9a at strains above roughly -1500 ppm and in Figure 9b at greater than roughly -300 ppm, is that increasing applied magnetic fields result in increasing Young's Moduli. Conversely, below these strains an increasing field results in decreasing moduli. This can be reconciled if one considers that the magnetostriction process in Terfenol-D occurs as magnetic moments are realigned from an "easy axis" (or energy minimization state) initially predominantly oriented at 90° or perpendicular to the transducer's applied field and external load to an easy axis within approximately 18° of the applied field orientation.⁹ Under compression of the Terfenol-D sample, (negative strains) an increasing axial magnetic field tries to move the magnetic moments away from the easy axis perpendicular to an external load, which makes the material "appear softer" to the external load. Hence an increased magnetic field would produce a lowered apparent modulus in compressed material. At the other extreme, as the sample is positively strained toward saturation and magnetic easy axes are within 18° of the applied field, an increasing axial magnetic field will act to resist jumping of magnetic moments back to the 90° easy axes, which makes the material appear stiffer to an external load. Hence an increased magnetic field would produce a higher apparent modulus in elongated or positively strained material.

BLOCKED FORCE Having examined the output characteristics of the transducer, the following discussion demonstrates a blocked force calculation at zero strain, where we are interested in quantifying and ultimately being able to predict the blocked force where $e(\mathbf{s}_0 + \mathbf{s}_B^H, H) = e(\mathbf{s}_0, 0)$. The transducer's blocked force output may be calculated using the maximum strain potential and modulus of elasticity relationship presented in Equation 2b. For convenience, the force results are normalized to stresses by dividing Equation 2b through by the cross-sectional area of the Terfenol-D core. Thus, the blocked stress \mathbf{s}_B^H is equal to Young's modulus E_Y^H times the maximum strain potential e_{max}^H as shown in Equation 3.

$$\mathbf{s}_B^H = \frac{F_B^H}{A} = E_Y^H e_{max}^H \quad (3)$$

Proceeding with the blocked stress calculation for the Figure 5 and 6 load lines, determining the maximum strain potential e_{max}^H is straightforward. The strain values may be picked off the x axis of the load line plots for a given applied field H . However, choosing the appropriate modulus of elasticity is not as straightforward. Referring to the modulus of elasticity plots in Figure 9, the modulus for a particular applied field varies significantly with both strain and preload \mathbf{s}_0 . Although we are considering the blocked stress at the initial transducer length (at zero strain) the modulus values over the range from zero to maximum strain are considered.

Figure 10 shows maximum value of the modulus and the modulus at zero strain (as determined from Figure 9a) in addition to a calculated modulus for the zero preload test case. The calculated modulus for each applied field is determined by dividing the blocked stress at $e(\mathbf{s}_0 + \mathbf{s}_B^H, H) = e(\mathbf{s}_0, 0)$ (as determined from Figure 5) by the maximum strain potential to obtain $E_{Bef}(\mathbf{e}, \mathbf{s}_0, H)$ (the effective blocked modulus at a specific strain and preload as a function of applied magnetic field). Using either the maximum or zero-strain modulus in Equation 3 results in an overestimate or an underestimate of the blocked stress respectively, except for the lowest two magnetic fields.

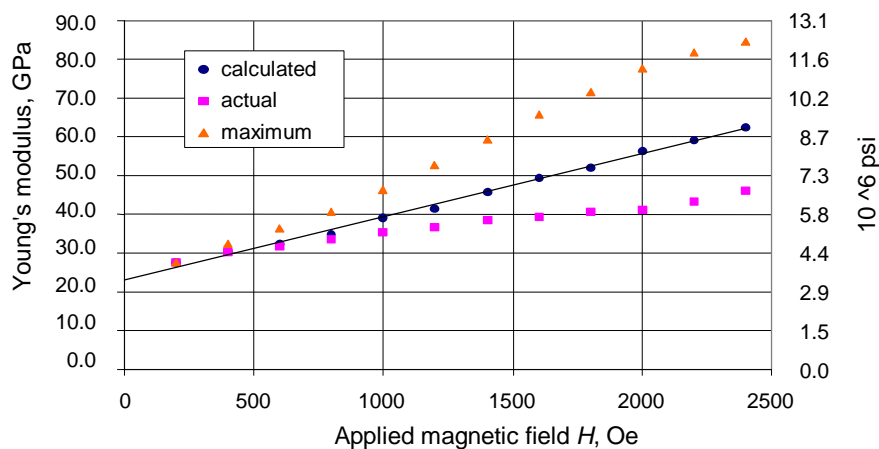


Figure 10. Elastic modulus values from the 0.0 MPa preload load line data.

An interesting observation is that the calculated moduli of Figure 10 are linearly dependent on the applied field. A least squares fit gives Equation 4 where $E_{Beff}(e, s_0, H)$ is the effective modulus (in Pascal) to be used in Equation 3 for predicting blocked forces and H is the applied field in Oe.

$$E_{Beff}(0,0, H) = [16.7 * 10^6 * H + 20.7 * 10^9] Pa \quad (4)$$

Figure 11 shows similar data on elastic moduli from the 6.9 MPa (1.0 ksi) preload load lines. The zero-strain moduli and calculated moduli are close in value. A polynomial fit of the calculated moduli for various applied magnetic fields yields the quadratic polynomial given by Equation 5.

$$E_{Beff}(0,6900, H) = [-1.16 * 10^4 * H^2 + 40.0 * 10^6 * H + 10^9] Pa \quad (5)$$

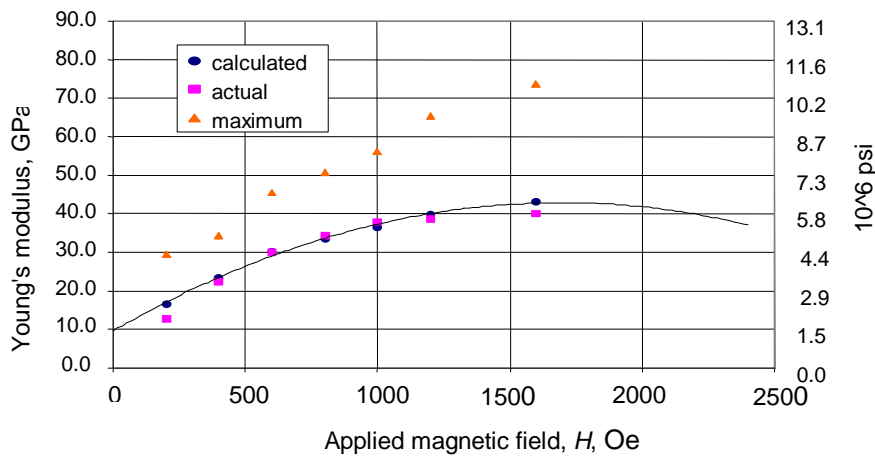


Figure 11. Elastic modulus values from the 6.9 MPa preload load line data.

SAMPLE CALCULATIONS A sample calculation follows to determine the blocked stress and force values at zero strain with an applied field of 1000 Oe. Results are for a zero preloaded transducer under quasi-static conditions where the field is applied prior to loading.

Applied field	1000 Oe
Terfenol-D cross-sectional area	31.7 mm ²
Observed maximum strain:	580*10 ⁻⁶ m/m
Observed blocked stress:	22.8 MPa (from Figure 5)
Observed blocked force	(22.8*10 ⁶ Pa)(31.7*10 ⁻⁶ m ²) = 722 N
Calculated blocked stress (Eq. 3,4)	((16.7*10 ⁶ Pa/Oe)(1000 Oe) + 20.7*10 ⁹ Pa)(586*10 ⁻⁶) = 21.9 MPa
Calculated blocked force	(21.9*10 ⁶ Pa) (31.7*10 ⁻⁶ m ²) = 694 N

When implementing blocked force results, one must also account for the stiffness of the load. Equation 6 gives the effective blocked force where the blocked stiffness of the Terfenol-D transducer driver k_B and stiffness of the load k_S are in series.

$$F_{Beff} = (k_B) e_{max}^H L \left[1 - \frac{k_B}{(k_B + k_S)} \right] \quad \text{where} \quad k_B = \frac{AE_{Beff}^H}{L} \quad (6)$$

with A is the cross sectional area, and L the length of the Terfenol-D driver. This correction was applied to the load line data presented to take into account test stand component compliance.

4. CONCLUSIONS

The output force-strain relationship of a Terfenol-D magnetostrictive transducer was presented in the form of load lines from test data obtained at constant temperature, under 0.0 and 6.9 MPa preloads, and for DC magnetic fields of up to 2400 Oe. This data was used to characterize the blocked force rating of the transducer under study and to examine the variability of the Terfenol-D transducer driver's elastic modulus with operating conditions. In addition, a discussion of equations that can be used in predicting transducer blocked force ratings and sample calculations were presented.

The blocked force rating of a Terfenol-D transducer is limited by the maximum magnetic field the transducer can supply. In addition, the initial stress or preload applied to the Terfenol-D driver has a significant impact on the blocked force achievable by the device, with a prestress of 6.9 MPa almost doubling the blocked force achieved with a zero preload in the same transducer for a given magnetic field. The sensitivity of the load lines to stress, strain and applied magnetic field suggests that optimization of a Terfenol-D transducer's force output will require knowledge of the range of expected operating conditions.

Both the 0.0 and 6.9 MPa preload data result in maximum values for the elastic modulus that lead to an over estimate of the blocked force or stress output capability. The zero strain modulus gives an underestimate of the blocked force for the 0.0 preload load line data, while actually mapping quite closely the modulus needed to predict the blocked force for the 6.9 MPa preload load line data. Empirical relations were identified for the effective modulus as a function of applied field H for both the 0.0 and 6.9 MPa preload conditions (Equations 4 and 5). These relationships and the maximum strain for a given applied magnetic field from Figures 5 or 6 can be used (in Equation 3) to predict the blocked force rating values for the transducer under study. Further study is warranted to ascertain how broadly applicable these specific relationships are to transducer designs having different magnetic circuit and thermal characteristics, and to investigate the effects of stress and magnetic history on load line characteristics.

ACKNOWLEDGEMENTS

The authors wish to acknowledge Nicholas Lapointe for his assistance in the data collection and Marcelo Dapino for his patience and advice. The NSF Division of Civil and Mechanical Systems provided financial support for this study.

REFERENCES

1. J. Butler, *Application Manual for the Design of Terfenol-D Magnetostrictive Transducers*, 1988, Edge Technologies, Ames, IA, 1988.
2. D. Jiles, *Introduction to Magnetism and Magnetic Materials*, pp 121-128, Chapman and Hall, London 1998.
3. V. Giurgiutiu, C.A. Rogers, "Power and energy characteristics of solid-state induced-strain actuators for static and dynamic applications", *Journal of Intelligent Material Systems and Structures*, Vol. 8, pp738-750, September 1997.
4. A.E. Clark, H.T. Savage, and M.L. Spano, "Effect of stress on the magnetostriction and magnetization of single crystal $Tb_{2.7}Dy_{7.3}Fe_2$ ", *IEEE Transactions on Magnetics*, **20**(5), pp1443-1445, 1984.
5. K. Mori, J. Cullen, A.E. Clark, "Magnetostriction in $Tb_{2.7}Dy_{7.3}Fe_2$: evidence for a low temperature transition," *IEEE Transactions on Magnetics*, **19**(5), September, 1983.
6. F. Claeysen, D. Boucher, and S. Faure, "Characterization of length expander magnetostrictive rare earth-iron rods under normal use conditions in transducers," *J. Acoust. Soc. Am. Suppl.* 1(83), September 20, 1988.

7. F. Calkins, *Design, Analysis, and Modeling of Giant Magnetostrictive Transducers*, pp 65-69, Iowa State University, Ames, Iowa, 1997.
8. H.T. Savage, A. E. Clark, and D. Pearson, The stress dependence of the ΔE effect in Terfenol-D, in material presented at the Fourth Joint MMM-Intermag Conference, Vancouver, Canada, 7/88.
9. M.J. Dapino, F.T. Calkins, A.B. Flatau, "On identification and analysis of fundamental issues in Terfenol-D transducer modeling", *Proc. of SPIE Smart Structures and Materials*, Vol. 3329, pp185-197, San Diego, CA, March 1998.
10. A.E. Clark, M.L. Spano, and H.T. Savage, "Effect of stress on the magnetostriction and magnetization of rare earth-Re_{1.95} alloys", *IEEE Transactions on Magnetics*, **19**(5), pp1964-1966, 1983.
11. M.B. Moffet, A.E. Clark, M. Wun-Fogle, J. Linberg, J.P. Teter, E.A. McLaughlin, "Characterization of Terfenol-D for magnetostrictive transducers", *J. Acoust. Soc. Am.*, 89(3), pp.1448-1454, March 1991.
12. A.E. Clark, J.B. Restorff, M. Wun-Fogle, and J.F. Lindberg, "Magnetoelastic coupling and the ΔE effect in TbxDy_{1-x} single crystals", *J. Appl. Phys.*, 73(10), pp. 6150-6151, May 1993.